Antiviral Research 165 (2019) 1–10

Contents lists available at ScienceDirect

Antiviral Research

journal homepage: www.elsevier.com/locate/antiviral

# Characterization of Reston virus infection in ferrets

Feihu Yan[a,b,c], Shihua He[a], Logan Banadyga[a], Wenjun Zhu[a], Huajun Zhang[b], Md Niaz Rahim[a,b], Brad Collignon[d], Chandrika Senthilkumaran[a], Carissa Embury-Hyatt[d], Xiangguo Qiu[a,b,*]

[a] Special Pathogens Program, National Microbiology Laboratory, Public Health Agency of Canada, Winnipeg, Manitoba, Canada
[b] Department of Medical Microbiology, University of Manitoba, Winnipeg, Manitoba, Canada
[c] Key Laboratory of Jilin Province for Zoonosis Prevention and Control in Key Lab, Changchun Veterinary Research Institute, Chinese Academy of Agricultural Sciences, Changchun, Jilin, China
[d] Canadian Food Inspection Agency, National Centre for Foreign Animal Disease, Winnipeg, Manitoba, Canada

ARTICLE INFO

*Keywords:*
Ebolavirus
Reston virus
Lethal disease
Ferret

ABSTRACT

Among the five currently recognized type viruses within the genus *Ebolavirus*, Reston virus (RESTV) is not known to cause disease in humans, although asymptomatic infections have been confirmed in the past. Intriguingly, despite the absence of pathogenicity in humans, RESTV is highly lethal to nonhuman primates and has been isolated from domestic pigs co-infected with other viruses in the Philippines and China. Whether infection in these animals can support the eventual emergence of a human-pathogenic RESTV remains unclear and requires further investigation. Unfortunately, there is currently no lethal small animal model available to investigate RESTV pathogenicity or pan-ebolavirus therapeutics. Here we show that wild type RESTV is uniformly lethal in ferrets. In this study, ferrets were challenged with 1260 $TCID_{50}$ of wild type RESTV either intramuscularly or intranasally and monitored for clinical signs, survival, virus replication, alteration in serum biochemistry and blood cell counts. Irrespective of the route of challenge, viremia occurred in all ferrets on day 5 post-infection, and all animals succumbed to infection between days 9 and 11. Additionally, several similarities were observed between this model and the other ferret models of filovirus infection, including substantial decreases in lymphocyte and platelet counts and abnormalities in serum biochemistry indicating hepatic injury. The ferret model represents the first uniformly lethal model for RESTV infection, and it will undoubtedly prove useful for evaluating virus pathogenicity as well as pan-ebolavirus countermeasures.

## 1. Introduction

Belonging to the family *Filoviridae* and the genus *Ebolavirus* (Kuhn et al., 2010), Reston virus (RESTV) causes a highly lethal disease in nonhuman primates (NHPs) but is non-pathogenic in humans (Burk et al., 2016). RESTV was first isolated in 1989 from cynomolgus macaques housed in a primate quarantine facility in Reston, Virginia, following their importation from the Philippines (Geisbert and Jahrling, 1990; Hayes et al., 1992). Subsequent cases in other animal facilities in Pennsylvania and Texas were linked to the import of macaques from the same exporting facility in the Philippines. Infected macaques developed a severe hemorrhagic illness that shared many clinical hallmarks with Ebola virus (EBOV) disease in humans, including bloody diarrhea and subcutaneous hemorrhaging (Jahrling et al., 1990, 1996). Additional cases of RESTV infection in macaques were once again reported in 1992 in a facility in Italy and in 1996 in Texas, all of which were linked to the same primate exporting facility in the Philippines (World Health Organization, 1992; Rollin et al., 1999). The original source of RESTV introduction to the exporting facility in the Philippines has never been identified (Miranda and Miranda, 2011). Notably, no animal handlers developed disease during any of these outbreaks, although several of them later became seropositive, indicating exposure had occurred (Barrette et al., 2009; Centers for Disease Control, 1990).

In 2008, the discovery of RESTV in pigs co-infected with porcine reproductive and respiratory syndrome (PRRS) virus in the Philippines raised fears of a potential threat to human health through the food chain (Marsh et al., 2011). Though the pig farmers and the abattoir workers did not show any clinical signs, six individuals who had daily occupational exposure to the pigs were seropositive for RESTV (Miranda and Miranda, 2011; Miranda et al., 1991), indicating possible pig-to-human transmission of RESTV. Although not proven, it was speculated that the virus could have been transmitted from bats to pigs,

* Corresponding author. Special Pathogens Program, National Microbiology Laboratory, Public Health Agency of Canada, 1015 Arlington Street, Winnipeg, MB, R3T 3R2, Canada.
*E-mail address:* xiangguo.qiu@canada.ca (X. Qiu).

https://doi.org/10.1016/j.antiviral.2019.03.001
Received 9 December 2018; Received in revised form 28 February 2019; Accepted 1 March 2019
Available online 02 March 2019

**Table 1**
Clinical findings for RESTV-infected ferrets. Fever is defined as a temperature above 39.8 °C. RR, Respiratory rate; dpi, day post infection; IM, intramuscular; IN, intranasal. ALT, alanine aminotransferase; TBIL, total bilirubin.

| Animal ID | Sex | Route of Infection | Clinical Signs (dpi) | | | Fever Onset (dpi) | Time of Death (dpi) | Clinical Score before Euthanasia | Other Important Findings (dpi) |
|---|---|---|---|---|---|---|---|---|---|
| | | | Depression | Increased RR | Dark Stool | | | | |
| 1487 | M | IM | 8 | 5 | 7 | 6 | 10 | 26 | Pale skin (10) |
| 1223 | M | IM | 7 | 5 | 7 | 5 | 11 | 22 | Found dead (11); ALT and TBIL levels were above the assay detection limit (11) |
| 1983 | F | IM | 7 | 7 | 7 | 6 | 9 | 28 | Splenomegaly (9) |
| 1282 | F | IM | 8 | 7 | 7 | 4 | 10 | 26 | _ |
| 1509 | M | IN | 10 | 5 | 10 | 6 | 10 | 26 | Pale skin (10) |
| 1002 | M | IN | 10 | 7 | 10 | 5 | 11 | 41 | _ |
| 1665 | F | IN | 10 | 7 | 10 | 4 | 10 | 28 | Pale skin (10) |
| 1240 | F | IN | 10 | 5 | 10 | 5 | 11 | 44 | _ |

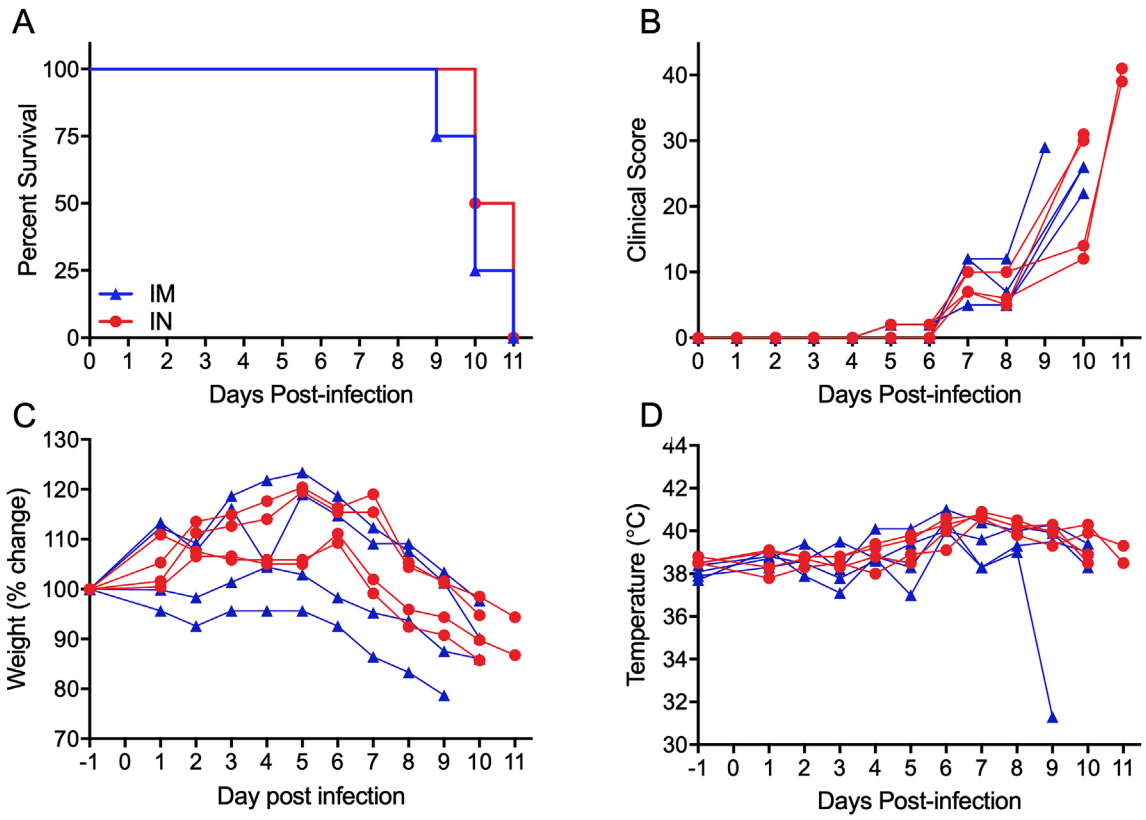


**Fig. 1.** Clinical findings of ferrets infected with RESTV. Ferrets were infected with RESTV either intramuscularly (IM; blue triangles) or intranasally (IN; red circles). Following infection, animals were monitored for survival (A), clinical signs of disease (B) weight change (C) and temperature (D). Individual values for clinical score, weight change, and temperature are indicated at each time point.

and the recent discovery of RESTV RNA in Philippine bats supports this speculation (Jayme et al., 2015). In 2012, a study revealed the presence of antibodies for RESTV among Chinese bat populations (Yuan et al., 2012), and following this report, RESTV was isolated from domestic pigs in China that died after showing typical clinical signs of PRRS (Pan et al., 2014). Interestingly, the RESTV variants isolated from the pigs in the Philippines were different in genome sequence from the original virus isolated in 1989 from the cynomolgus macaques (Albarino et al., 2017), suggesting a certain amount of plasticity within the genome. The continued circulation of RESTV in reservoir species or other hosts may result in the emergence of human-pathogenic RESTV variants, although the probability of such a scenario is unclear and may depend on a range of poorly-understood factors (Cantoni et al., 2016).

Unfortunately, the pathogenesis of RESTV and its potential to cause disease in humans has been poorly characterized, mainly because studies are currently limited to the NHP animal model. No uniformly lethal small animal model currently exists for RESTV. Ferrets are popular and useful animals for studying the transmission and pathogenesis of many emerging viruses (Enkirch and von Messling, 2015), and they have been successfully used to develop lethal models for three other ebolaviruses: EBOV, Sudan virus (SUDV) and Bundibugyo virus (BDBV) (Cross et al., 2016; Kozak et al., 2016; Kroeker et al., 2017). In the present study, we demonstrate that ferrets are also susceptible to wild type RESTV infection, and develop a uniformly lethal disease that is similar to what is observed in NHPs. Thus, this research demonstrates that ferrets are not only a valuable small animal model for characterizing RESTV pathogenesis, but it also provides a platform for vaccine and antibody development against RESTV and pan-ebolavirus therapeutics.

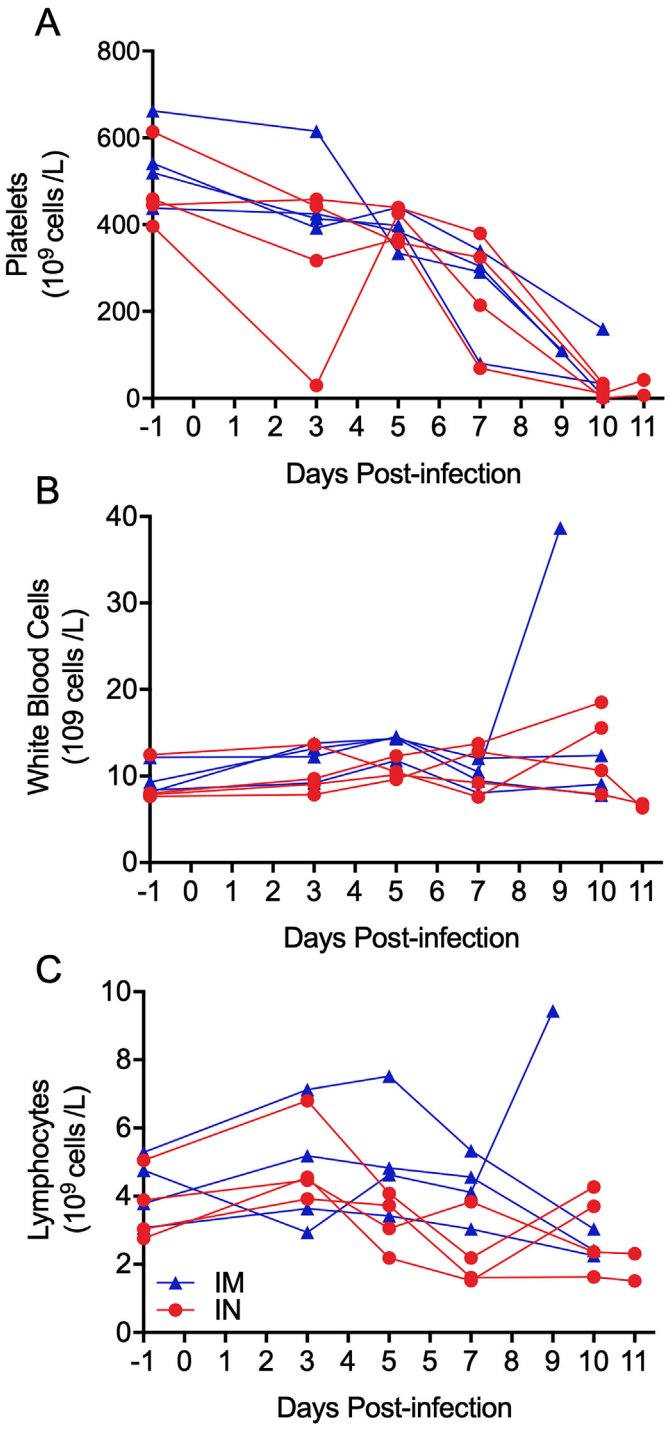


**Fig. 2.** Hematology parameters in RESTV-infected ferrets. Platelets (A), white blood cells (B) and lymphocytes (C) were quantified from whole blood using the Abaxis HM5 system. Ferrets were infected with RESTV intramuscularly (IM; blue triangles) or intranasally (IN; red circles), and the individual values for each parameter is indicated at each time point.

## 2. Materials and methods

### 2.1. Ethics statement

The animal work for this study was performed in the biosafety level-4 (BSL-4) facility at the Canadian Science Centre for Human and Animal Health (CSCHAH) in Winnipeg, Canada. All work with live animals was approved by the institutional Animal Care Committee in accordance with guidelines from the Canadian Council on Animal Care. Animals were acclimatized for 7 days prior to infection, given food and water *ad libitum* and monitored twice daily. Environmental enrichment was also provided in the cages during the study.

### 2.2. Virus

RESTV (Reston virus/M. fascicularis-tc/USA/1990/Philippines89-AZ1435) was obtained from the Centers for Disease Control and Prevention (Atlanta, GA) with an unknown passage history. Virus was passaged a single time on Vero E6 cells (ATCC) to generate a working stock. Sequencing revealed that the working stock of virus was approximately 99% identical to the RESTV reference sequence (GenBank # KY008770.1), with only 17 nucleotide changes observed (Supplemental Table 1).

### 2.3. Animals

Eight six-month old male and female ferrets (*Mustela putorius furo*) were purchased from Marshall BioResources (New York, USA). Each ferret was implanted with an IPTT-300 temperature and ID transponder (BioMedic Data Systems Inc., USA) subcutaneously over the dorsal aspect of the caudal region. After a week of acclimatization, equal numbers of female and male ferrets were randomly assigned into two groups and infected either intramuscularly (IM) or intranasally (IN) with RESTV with a target dose of 1000 TCID50 (back-titered to 1260 $TCID_{50}$). After challenge with the virus, all the animals were monitored daily for signs of disease, including change in body weight, temperature (via transponder reading), physical activity, and food and water intake (Supplemental Fig. 1). Oral and rectal swabs, nasal washes and blood samples were collected on days −1, 3, 5, 7, 9 and at terminal time points until the end of the experiment to evaluate viral shedding and serum biochemistry. Lithium heparin blood samples were collected to analyze serum biochemistry and EDTA blood samples were collected for complete blood count. Tissues (liver, spleen, kidney and lung) were collected during necropsy for virus detection and histopathological evaluation.

### 2.4. Plasma biochemistry and blood counts

Plasma biochemistry was evaluated with the VetScan VS2 blood analyzer (Abaxis, USA) using heparinized blood. Evaluation of complete blood counts was done using a VetScan HM5 hematology system (Abaxis, USA) with the whole blood collected in EDTA tubes. All analyses were done according to the manufacturer's instructions.

### 2.5. Quantification of viral loads by RT-qPCR

Total RNA was extracted from blood, oral and rectal swabs and nasal washes, using the QIAamp Viral RNA Mini kit (Qiagen). Tissues were homogenized in PBS using a Precellys® lysing kit according to the manufacturer's protocol (BERTIN Corp. MD, USA), and total RNA was extracted using the RNeasy Kit according to the manufacturer's instructions (Qiagen). Presence of RESTV RNA in blood, oral and rectal swabs, nasal washes, and tissues was evaluated by reverse transcription-quantitative PCR (RT-qPCR) targeting the RESTV NP gene using Roche Lightcycler 480 RNA Master Hydrolysis Probes kit with the following primers and probes: RESTV-N-forward (5′-CACGAAGAGGACA CCCTTATG-3′), RESTV-N-reverse (5′-CGGGATCTTGTTGGCTACTT-3′), RESTV-N-probe (5'-/56-FAM/CCTCAAGCT/ZEN/TACCTCCGCTGG AAT/3IABkFQ/-3′). The cycling conditions were as follows: 63 °C for 3 min, 95 °C for 30 s, followed by 45 cycles of 95 °C for 15 s, 60 °C for 30 s. Positive results were defined by a cycle threshold value of ≤ 36.

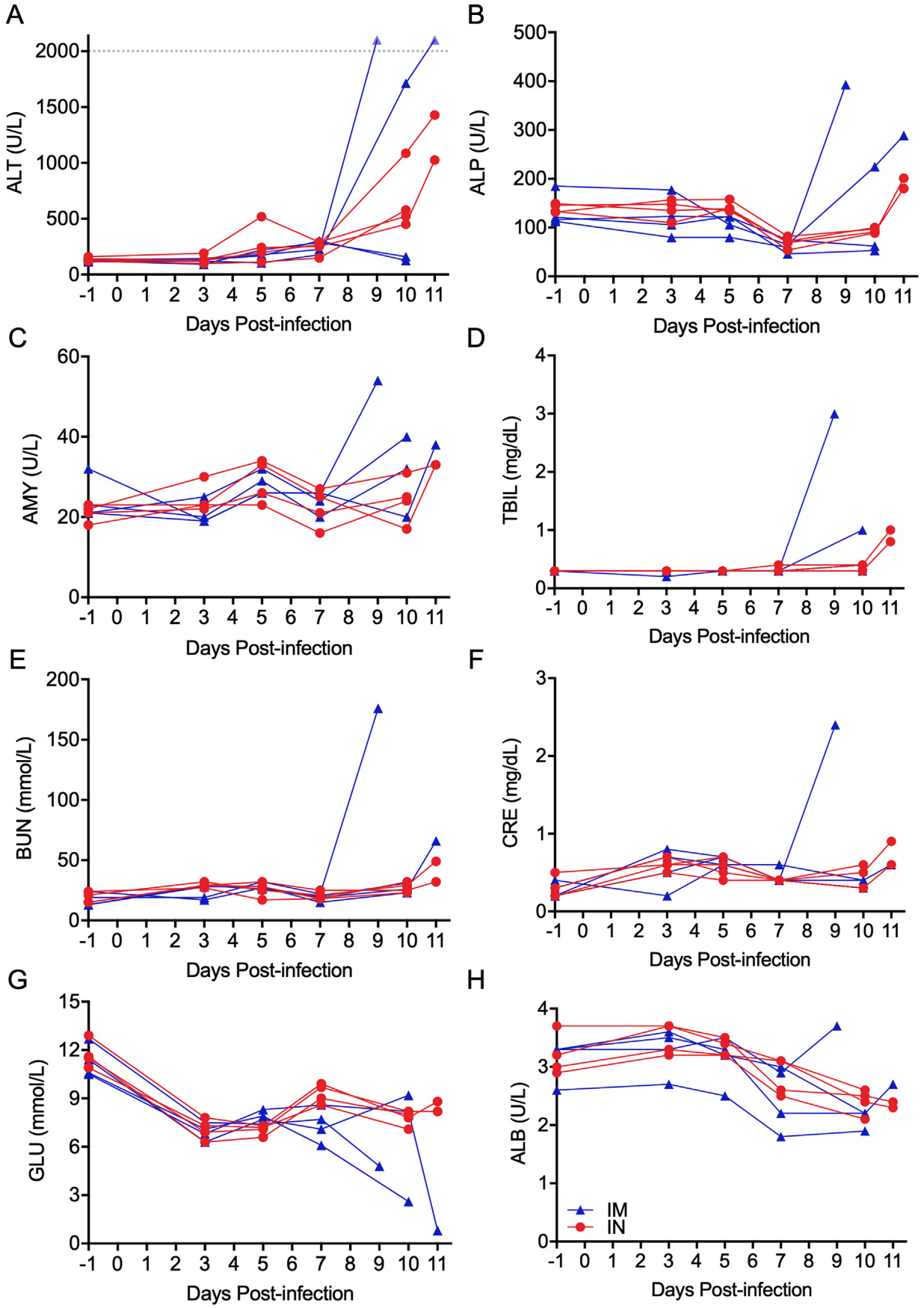


**Fig. 3.** Blood biochemistry in RESTV-infected ferrets. (A–H) Blood levels for alanine aminotransferase (ALT; A), alkaline phosphatase (ALP; B), amylase (AMY; C), total bilirubin (TBIL; D), blood urea nitrogen (BUN; E), creatine (CRE; F), glucose (GLU; G), serum albumin (ALB; H). Ferrets #1983 and #1223 had ALT levels above the assay detection limit (grey dashed line) on 9 and 11 dpi, respectively. Ferrets were infected with RESTV intramuscularly (IM; blue triangles) or intranasally (IN; red circles), and the individual values for each parameter is indicated at each time point.

**Table 2**
Detection of RESTV RNA in blood, swabs (rectal and oral) and nasal washes in ferrets infected with RESTV via the intramuscular route. GEQ; genome equivalent; $TCID_{50}$, tissue culture infective dose; -, not detected; ND, not done; x, animal dead.

| Animal | Day 3 | | Day 5 | | Day 7 | | Day 9 | | Day 10 | | Day 11 | |
|---|---|---|---|---|---|---|---|---|---|---|---|---|
| ID | GEQ/ml | $TCID_{50}$/ml | GEQ/ml | $TCID_{50}$/ml | GEQ/ml | $TCID_{50}$/ml | GEQ/ml | $TCID_{50}$/ml | GEQ/ml | $TCID_{50}$/ml | GEQ/ml | $TCID_{50}$/ml |
| 1487 | | | | | | | | | | | | |
| Blood | 3.56E03 | 1.78E03 | 2.99E07 | 3.16E03 | 1.78E08 | 3.16E03 | ND | ND | 3.76E08 | 1.78E04 | x | x |
| Nasal | – | – | 4.23E04 | – | 6.62E05 | 3.16E02 | ND | ND | 5.97E07 | 3.16E02 | x | x |
| Oral | – | – | 1.81E04 | – | 5.71E06 | 3.16E02 | ND | ND | 4.94E08 | 3.16E02 | x | x |
| Rectal | – | – | 5.97E04 | 3.16E02 | 1.29E06 | 3.16E02 | ND | ND | 4.03E06 | 3.16E02 | x | x |
| 1223 | | | | | | | | | | | | |
| Blood | 1.88E04 | 1.78E03 | 4.61E07 | 1.00E05 | 5.69E08 | 5.62E04 | ND | ND | 1.02E10 | 3.16E07 | 5.18E08 | 1.78E04 |
| Nasal | – | – | 2.59E04 | 3.16E02 | 1.33E07 | 3.16E02 | ND | ND | 1.19E07 | 1.78E04 | 6.40E07 | 5.62E04 |
| Oral | – | – | 7.58E04 | – | 8.86E07 | 3.16E02 | ND | ND | 3.40E08 | 3.16E02 | 4.88E09 | 3.16E02 |
| Rectal | – | – | 3.63E04 | – | 8.23E04 | 3.16E02 | ND | ND | 2.63E07 | 3.16E02 | 3.14E08 | 3.16E02 |
| 1983 | | | | | | | | | | | | |
| Blood | 1.56E04 | 3.16E03 | 5.55E07 | 5.62E03 | 9.18E08 | 5.62E05 | 5.38E08 | 1.78E10 | x | x | x | x |
| Nasal | – | – | 5.49E04 | 3.16E02 | 1.17E08 | 3.16E02 | 3.82E07 | 3.16E02 | x | x | x | x |
| Oral | – | – | 6.13E04 | 3.16E02 | 1.42E07 | 3.16E02 | 6.89E07 | 3.16E02 | x | x | x | x |
| Rectal | – | – | 5.11E04 | – | 2.94E05 | 1.78E02 | 3.52E07 | 3.16E02 | x | x | x | x |
| 1282 | | | | | | | | | | | | |
| Blood | 3.58E03 | 1.78E04 | 2.45E07 | 1.78E03 | 9.91E07 | 3.16E04 | ND | ND | 4.25E08 | 5.62E03 | x | x |
| Nasal | – | – | 5.73E04 | – | 1.66E06 | 3.16E02 | ND | ND | 4.36E07 | 3.16E02 | x | x |
| Oral | – | – | 2.95E04 | 3.16E02 | 2.63E06 | 3.16E02 | ND | ND | 2.90E07 | 3.16E02 | x | x |
| Rectal | – | – | 2.75E04 | – | 1.73E04 | – | ND | ND | 1.02E07 | 3.16E02 | x | x |

**Table 3**
Detection of RESTV RNA in blood, swabs (rectal and oral) and nasal washes in ferrets infected with RESTV via the intranasal route. GEQ, genome equivalent; $TCID_{50}$, tissue culture infective dose; -, not detected; ND, not done; x, animal dead.

| Animal | Day 3 | | Day 5 | | Day 7 | | Day 10 | | Day 11 | |
|---|---|---|---|---|---|---|---|---|---|---|
| ID | GEQ/ml | $TCID_{50}$/ml | GEQ/ml | $TCID_{50}$/ml | GEQ/ml | $TCID_{50}$/ml | GEQ/ml | $TCID_{50}$/ml | GEQ/ml | $TCID_{50}$/ml |
| 1509 | | | | | | | | | | |
| Blood | – | – | 6.62E05 | 3.16E03 | 1.10E08 | 5.62E05 | 6.22E09 | 3.16E06 | x | x |
| Nasal | – | – | 3.64E04 | – | 4.63E05 | 3.16E02 | 5.84E09 | 1.78E03 | x | x |
| Oral | 3.36E05 | 3.16E02 | 2.51E04 | – | 1.18E07 | 3.16E02 | 4.45E08 | 3.16E03 | x | x |
| Rectal | – | – | 1.22E06 | 3.16E02 | 3.43E06 | 3.16E02 | 7.27E06 | 5.62E02 | x | x |
| 1002 | | | | | | | | | | |
| Blood | – | – | 4.07E06 | 3.16E03 | 3.65E08 | 5.62E05 | 1.47E09 | 3.16E05 | 5.62E07 | ND |
| Nasal | – | – | 6.07E06 | 3.16E02 | 2.04E05 | 3.16E02 | 8.47E06 | 5.62E02 | 3.16E02 | ND |
| Oral | – | – | 1.56E06 | 3.16E02 | 1.54E06 | 3.16E02 | 6.29E08 | 3.16E02 | 3.16E02 | ND |
| Rectal | – | – | 2.89E04 | – | 1.43E05 | 3.16E02 | 7.59E06 | 3.16E02 | 3.16E02 | ND |
| 1665 | | | | | | | | | | |
| Blood | – | – | 1.39E04 | 3.16E03 | 4.03E08 | 1.78E05 | 6.77E09 | 1.00E07 | x | x |
| Nasal | 2.29E05 | – | 3.17E04 | 1.78E02 | 2.57E05 | 3.16E02 | 5.18E09 | 3.16E02 | x | x |
| Oral | – | – | 8.57E05 | 3.16E02 | 1.63E07 | 3.16E02 | 3.08E06 | 1.78E03 | x | x |
| Rectal | 3.13E03 | 3.16E02 | 6.98E04 | 3.16E02 | 1.23E04 | – | 3.68E07 | 3.16E02 | x | x |
| 1240 | | | | | | | | | | |
| Blood | – | – | 9.53E06 | 3.16E03 | 1.30E09 | 5.62E05 | 3.06E10 | 1.78E07 | 2.60E10 | 5.62E07 |
| Nasal | 2.84E04 | – | 4.63E05 | – | 4.18E07 | 3.16E02 | 9.26E07 | 3.16E02 | 5.65E07 | 3.16E02 |
| Oral | 3.07E04 | 3.16E02 | 7.83E04 | 3.16E02 | 1.19E08 | 3.16E02 | 1.30E08 | 3.16E02 | 1.37E07 | 5.62E02 |
| Rectal | 3.95E03 | 5.62E02 | – | – | 6.20E04 | 3.16E02 | 9.36E06 | 3.16E02 | 5.70E06 | 3.16E02 |

### 2.6. Quantification of viral loads by $TCID_{50}$

Samples (whole blood, oral and rectal swabs, nasal washes and tissues) that were positive for RT-qPCR were tested for live virus by $TCID_{50}$ assay. Vero-E6 Cells were infected with 10-fold serial dilutions of samples and incubated for 1 h at 37 °C with 5% $CO_2$. Then the inoculum was removed and the cells were overlaid with fresh DMEM containing 2% FBS. At 14 days post-infection, the plates were assessed for the lowest dilution at which 50% of the wells exhibited cytopathic effect. The $TCID_{50}$ was calculated according to the Reed-Muench method.

### 2.7. Whole-genome sequencing of RESTV

Viral RNA was extracted from whole blood obtained from animal #1059 at the terminal time point (10 dpi) using a Qiagen Viral RNA Mini kit, according to the manufacturer's instructions. Reverse transcription was carried out using the SuperVilo enzyme (ThermoFisher, USA) following the manufacturer's instructions. Four microliters of RNA were used in the reaction along with 250 ng of random hexamers (ThermoFisher, USA). The subsequent PCR reactions were carried out using CloneAmp HiFi PCR Premix (Clontech, USA) in 25 µl, using 4 µl of the RT product as template, primers at 200 nM, and 12.5 µl CloneAmp HiFi PCR Premix. The PCR conditions were 35 cycles as follows: 98 °C for 30 s, 98 °C for 10 s, 65 °C for 15 s, 72 °C for 1 min 30 s, and a final extension at 72 °C for 10 min. The amplicons were quantified using the PicoGreen dye and fragments from the same passage were pooled at equimolar concentration using a BioMek FX (BioTek). Library construction was done using the Nextera DNA XT Sample preparation kit (24-Sample) (Illumina) as per manufacturer's instructions. Sequencing was carried out using a MiSeq sequencer (Illumina) using the MiSeq Reagent Kit v3 (600 cycles) (Illumina). Paired reads from each passage

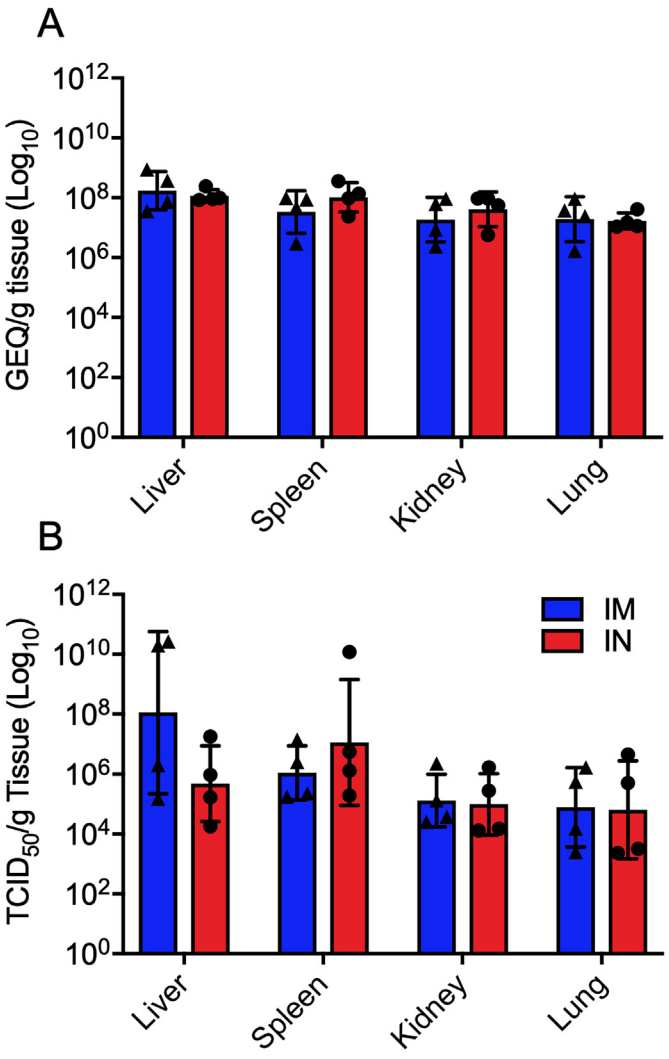


**Fig. 4.** Detection of RESTV RNA and infectious virus in tissues. Tissues (liver, spleen, kidney, and lung) were collected during necropsy, after which RESTV RNA levels were determined by RT-qPCR (A) and virus titers were determined by $TCID_{50}$ (B). Ferrets were infected with RESTV intramuscularly (IM) or intranasally (IN). The average value for each parameter is indicated by a blue (IM) or red (IN) column and individual values are indicated by triangles (IM) or circles (IN).

were aligned to a reference sequence (GenBank accession NC_004161) using Bowtie 2 version 2.0.5. Conversion to bam files, sorting, and indexing were performed using Samtools version 0.1.18. Freebayes version 0.9.8 was used to perform variant calling following a max complex gap of 0, a ploidy of 4, a minimum frequency of 10%, a minimum coverage of 1000 fold, a minimum quality score of 30, and to ignore deletions and insertions. The frequencies of variants were determined as the number of reads with a specific variant over the depth at that location. The coverage was confirmed by bedtools version 2.25.0.

### 2.8. Data analysis

Figures were generated using GraphPad Prism 6.0 software. Differences between means were evaluated using the paired, two-tailed, Student *t*-test and were deemed significant at P values of 0.05. Kaplan-Meier survival curves were analyzed by the log rank test.

### 2.9. Histopathology and immunohistochemistry

Tissues were fixed in 10% phosphate-buffered formalin, embedded in paraffin using standard procedures, sectioned at 5 µm, and stained with hematoxylin and eosin (H&E) for histopathologic examination as previously described (Kozak et al., 2016; Kroeker et al., 2017). For immunohistochemistry (IHC), paraffin-embedded tissue sections were quenched for 10 min in aqueous 3% hydrogen peroxide. Antigen retrieval was performed by pre-treating the tissues with proteinase K for 10 min. In-house generated primary anti-RESTV NP mAb-clone 7E7 (data unpublished) was used at a dilution of 1:400 (30 min incubation) to detect RESTV antigen in tissues. Sections were visualized using a horseradish peroxidase-labeled polymer, Envision system (anti-rabbit) (Dako, USA), subjected to reaction with the chromogen diaminobenzidine (DAB), and counterstained with Gill's hematoxylin.

## 3. Results

### 3.1. Clinical findings

Two groups of four ferrets were inoculated with RESTV at a dose of 1260 $TCID_{50}$ via either IM or IN route. After virus inoculation, ferrets in both groups were monitored for clinical signs of RESTV disease as well as survival. Samples collected during the experiment were evaluated for virus replication, plasma biochemistry and hematological parameters. Tissue samples collected during necropsy were analyzed by histopathology and immunohistochemistry.

The clinical findings are summarized in Table 1. All ferrets in both groups (IM and IN) were equally susceptible to infection with wild type RESTV and died or were euthanized between days 9 and11 post-infection (Fig. 1A). An increase in clinical score was observed beginning at 5 days post-infection (dpi) in animals that were IM inoculated (Fig. 1B), with animals exhibiting labored breathing, decreased activity and decreased food and water intake. Clinical scores increased on 7 dpi for animals in both the IM and IN group, and continued to increase for the duration of the experiment. By 10 dpi, 5 out of the 8 animals had reached a clinical score of 20 or above and were euthanized according to the predefined humane endpoint. One of the last three animals (#1223) succumbed to disease on 11 dpi, and the remaining two, both in the IN group, were euthanized. Weight loss (Fig. 1C) was first observed at 6 dpi in both groups, and animals continued to lose weight until the end of the experiment. Elevated temperature (Fig. 1D) was first observed in both groups at 4 dpi and peaked at 6 dpi for the IM group and 7 dpi for the IN group. Animal #1983 from the IM group showed hypothermia (31.3 °C) at 9 dpi and was euthanized at that time. None of these parameters (percent survival, weight change, clinical score and temperature) were significantly different between the two groups.

### 3.2. Hematology and plasma biochemistry

Hematological analysis revealed a decline in platelet count beginning on 3 dpi in both groups and continuing with the advancement of disease (Fig. 2A). A slight increase in white blood cell (WBC) counts (Fig. 2B) and lymphocyte counts (Fig. 2C) was observed in most of the ferrets at 3 dpi and 5 dpi. Notably, ferret #1983 had very high levels of WBCs and lymphocytes on 9 dpi, coincident with hypothermia and a clinical score of 29.

Changes in several plasma biochemistry markers are shown in Fig. 3. Plasma alanine aminotransferase (ALT) (Fig. 3A) started to increase in all the ferrets by 5–7 dpi, and by 10 dpi, 5 out of 7 animals showed a more than 3-fold increase. Ferret #1983, which was euthanized on 9 dpi, and ferret #1223, which was found dead on 11 dpi, both had serum ALT levels above the upper detection limit of the assay (points not shown in the graph) at their terminal time points. Plasma alkaline phosphatase (ALP) levels (Fig. 3B) decreased by more than 50% of their normal physiological level by 7 dpi in all the ferrets but started to increase by 10 dpi. Plasma levels of amylase (AMY; Fig. 3C), blood urea nitrogen (BUN; Fig. 3E) and creatinine (CRE; Fig. 3F)

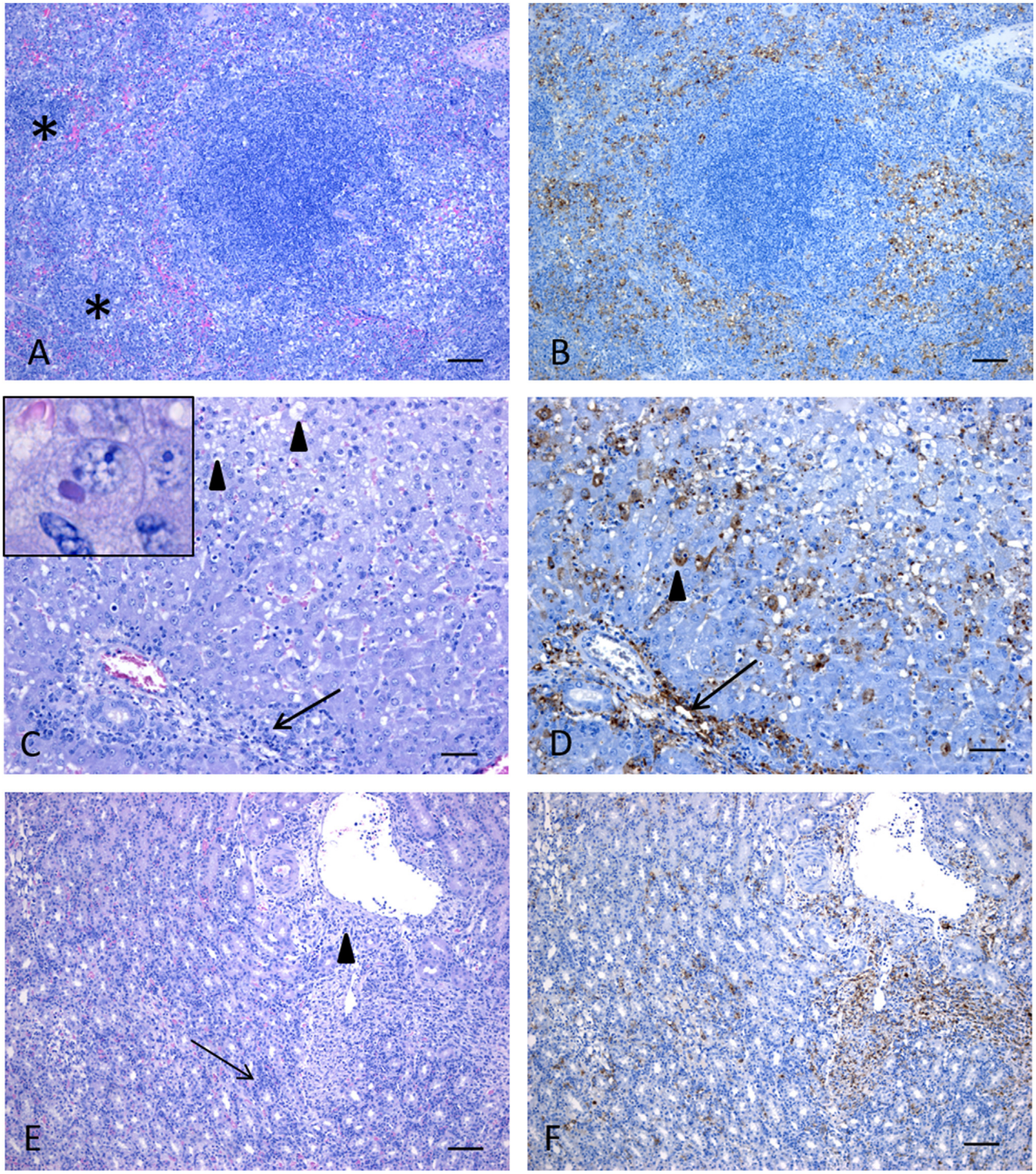


**Fig. 5.** Histopathology and immunohistochemistry findings in spleen, liver, and kidney from RESTV-infected ferrets. (A) Splenic cords are expanded by an increase in macrophages, neutrophils and lymphocytes (*). (B) Abundant viral antigen is detected primarily in red pulp areas of the spleen. (C) In the liver there is infiltration of portal areas with inflammatory cells (arrow) and multifocal vacuolation and degeneration of hepatocytes (arrowheads). Inset: Hepatocyte cytoplasmic viral inclusion body. (D) Positive immunostaining in the liver within portal areas (arrow) and individual hepatocytes (arrowhead). (E) Kidney lesions included perivascular inflammation (arrowhead) and interstitial nephritis (arrow). (F) Positive immunostaining was associated with the kidney lesions. Ferret #1665: A, B; ferret #1240: C, D; ferret #1002: E, F. A, B, E, F scale bar = 100 μm; C, D scale bar = 50 μm.

increased later during infection, around 10 dpi. Total bilirubin (TBIL; Fig. 3D) was stable until 9–10 dpi, when increases were observed. Blood glucose (Fig. 3G) and albumin (ALB; Fig. 3H) levels fluctuated during the course of infection and fell to levels 2–3 times lower than their physiologically normal levels before euthanasia. None of these values were significantly different between the IN and IM group.

### 3.3. Virus shedding and spread to internal organs

RESTV replication in blood and tissues, and shedding in oral and rectal swabs and nasal washes were evaluated by RT-qPCR, and quantification of infectious virus ($TCID_{50}$) was carried out with the samples that were positive by RT-qPCR (Tables 2 and 3). Viremia was first

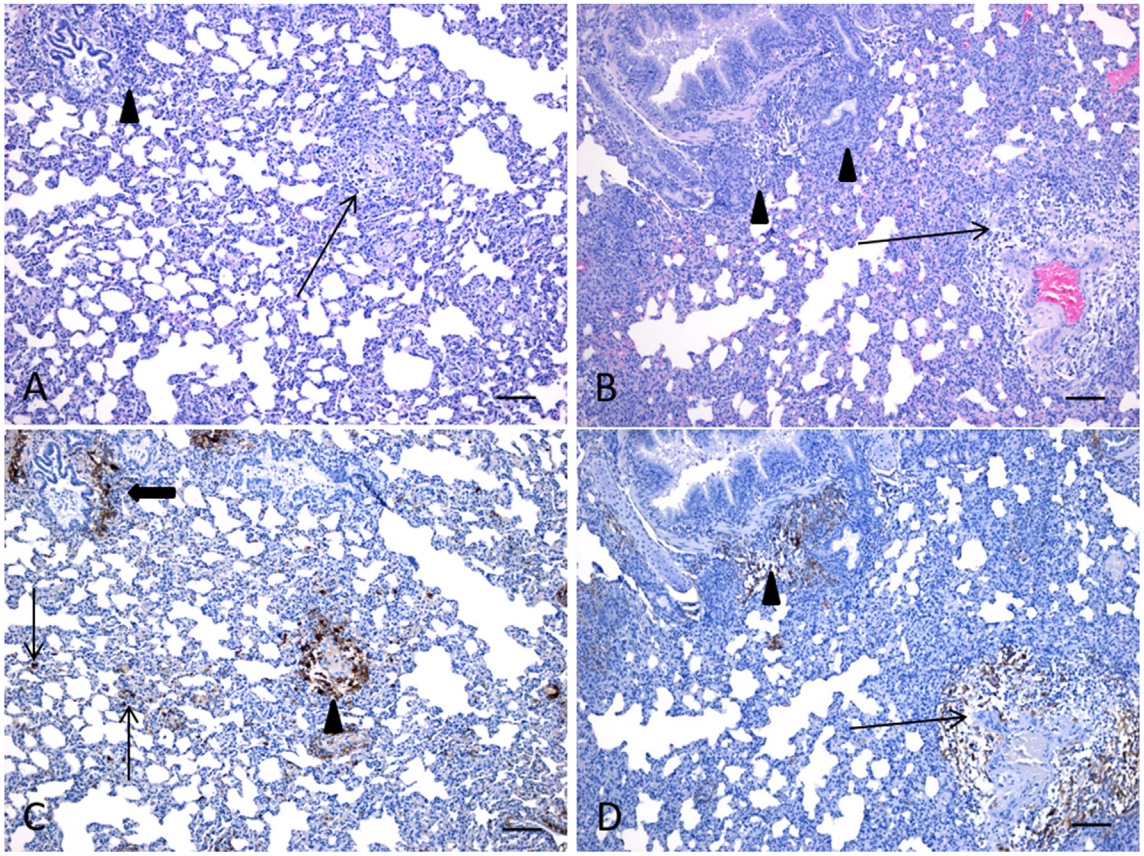


**Fig. 6.** Histopathology and immunohistochemistry findings in lungs from RESTV-infected ferrets. (A) In this lung there is mild expansion of the alveolar walls by infiltration of inflammatory cells as well as mild perivascular (arrow) and peribronchiolar (arrowhead) inflammation. (B) In this lung there is extensive peribronchiolar inflammation (arrowhead) and perivascular edema and inflammation (arrow). Note also the expansion of alveolar walls due to inflammatory cell infiltration. (C) Viral antigen is detected in scattered cells within alveolar walls (thin arrows) as well as in perivascular (thick arrow) and peribronchiolar (arrowhead) areas. (D) Positive immunostaining primarily in perivascular (arrow) and peribronchiolar (arrowhead) areas. Ferret #1223: A, C; ferret #1487: B, D. A, B, C, D scale bar = 100 μm.

detected at 3 dpi in the IM-inoculated group and at 5 dpi in the IN-inoculated group, although the RNA load at this timepoint was at least 10 times less than what was observed in the IM-inoculated group. By 7 dpi, viral RNA levels were similarly high in both groups and peaked around 10 dpi. RNA was detected in oral and rectal swabs, as well as nasal washes, as early as 3 dpi for the IN-inoculated group, suggesting virus shedding. Virus shedding was observed for the first time in the IM-inoculated group on 5 dpi, and it increased in both groups until the end of the experiment. Infectious virus was successfully isolated from samples that had high copy numbers of viral RNA (Tables 2 and 3). Tissues (liver, spleen, kidneys and lungs) harvested during necropsy were also evaluated for RESTV RNA by RT-qPCR, and both groups had very high copy numbers ($10^6$-$10^9$ GEQ/gram) of viral RNA in all tissues analyzed (Fig. 4A). Accordingly, infectious virus was detected in all tissues (Fig. 4B).

### 3.4. Histopathology and immunohistochemistry

In both the IN- and IM-inoculated groups, several histopathologic changes were observed in tissues that were associated with the presence of RESTV antigen. In all spleens of both groups, extensive expansion of the splenic cords with scattered necrotic cells was observed, as well as an increase in macrophages, neutrophils and lymphocytes (Fig. 5A). In two spleens lymphocytolysis was evident (not shown). Viral antigen was detected in the spleens of all animals, primarily within the red pulp, and was often observed within cells that morphologically appeared to be macrophages (Fig. 5B). Mild to severe pathology was observed in the livers of both groups. Prominent lesions included multifocal areas of vacuolar degeneration and loss of hepatocytes that were occasionally associated with neutrophil infiltration as well as infiltration of inflammatory cells into the portal areas (Fig. 5C). In a few of the livers, cytoplasmic viral inclusion bodies were observed (Fig. 5C, inset). Viral antigen could be detected in the livers of all animals within hepatocytes and in periportal areas (Fig. 5D). Kidney lesions were variable between individual animals but were similar in both IM and IN groups. The most consistently observed lesions included interstitial nephritis associated with necrotic cells and scattered epithelial tubular degeneration (Fig. 5E). Perivascular inflammation was also observed in most kidneys (Fig. 5E). Viral antigen could be detected in all animals primarily in perivascular areas as well as within the interstitium and was associated with inflammatory cells (Fig. 5F). Occasionally viral antigen could be detected within tubule epithelial cells. Lung lesions were variable between individual animals but similar in both groups. The most consistent lesion was mild to moderate expansion of the alveolar walls by infiltration of inflammatory cells (macrophages, neutrophils) with scattered necrotic cells (Fig. 6A). Often associated with this lesion was mild perivascular and peribronchiolar inflammation (Fig. 6A). In two of the animals (one IN- and one IM-inoculated) extensive peribronchiolar inflammation and perivascular edema and inflammation was observed (Fig. 6B). Viral antigen could be detected in scattered cells within alveolar walls (Fig. 6C) but was primarily observed in perivascular and peribronchiolar areas (Fig. 6C and D).

## 4. Discussion

Ferrets have proven to be useful model systems for a variety of other

viruses, particularly influenza virus, thanks to their relatively small body size and their similarity to humans, with regards to various aspects of their physiology, anatomy and metabolism. Recently, we and others developed the ferret model for wild type EBOV, BDBV, and SUDV infection, demonstrating that this animal model holds particular value for the filovirus research field (Cross et al., 2016; Kozak et al., 2016; Kroeker et al., 2017). Here, we demonstrate that wild type RESTV also causes severe disease in ferrets, recapitulating many of the clinical hallmarks of disease observed in NHPs. Both IM and IN routes of inoculation caused viremia at 5 dpi and resulted in 100% mortality, with a median survival time of 10 days. Uncontrolled viral replication was observed in the blood and major organs, and virus shedding was detected in oral and rectal swabs, as well as nasal washes, starting from 3 dpi. The immunohistochemistry findings were consistent with the virus detection in tissues. Furthermore, the depletion of platelets (thrombocytopenia), reduction in WBC and lymphocyte counts (lymphopenia), and disturbances in liver enzyme levels correlate with viral dissemination and organ failure, and reflect what is observed in the other ebolavirus ferret models (Cross et al., 2016; Kozak et al., 2016; Kroeker et al., 2017). Interestingly, however, in contrast to EBOV and BDBV infection in ferrets, RESTV infection, like SUDV infection, did not produce an obvious petechial rash, which is sometimes associated with filovirus disease. Similarly, whereas EBOV and BDBV infection resulted in only sporadic shedding of virus, RESTV and SUDV infection resulted in consistent virus shedding that continued until death.

NHPs are highly susceptible to RESTV, and RESTV studies have therefore primarily been limited to this model system (Jahrling et al., 1996). Although NHPs are the gold-standard model for studying filovirus pathogenesis and antiviral therapeutics, primary evaluation in small animal models prior to NHPs is typically carried out for ethical, practical, and economic reasons (Banadyga et al., 2018). Indeed, using small animal models to study disease pathogenesis allows more work to be performed in less sentient animals. Several small animal models have been developed by us and others to study filovirus infections and evaluate antiviral therapeutics and vaccines against those infections; however, besides the ferret model reported here, no immunocompetent, uniformly lethal small animal model has been described for RESTV (Banadyga et al., 2018; Siragam et al., 2018).

A previous study examined RESTV infection in several rodent models, including BALB/c and STAT1$^{-/-}$ mice, Hartley guinea pigs, and Syrian golden hamsters (de Wit et al., 2011). Of all rodents analyzed, only STAT1$^{-/-}$ mice showed clinical signs of disease, and RESTV variant Pennsylvania (but not variant 08-A) resulted in 50% lethality. Interestingly, unlike the ferrets, none of the rodents, including the STAT1$^{-/-}$ mice, shed virus in nasal and oropharyngeal swabs. Moreover, although RESTV replication in tissues was observed in STAT1$^{-/-}$ mice, guinea pigs and hamsters, the virus was eventually cleared fully or partially in guinea pigs and hamsters. The authors suggest that the absence of disease manifestation and controlled viral replication in BALB/c mice, guinea pigs, and hamsters may resemble human RESTV infection, while disease observed in STAT1$^{-/-}$ mice may more closely resemble RESTV infection in cynomolgus macaques. Likewise, the ferret model described here recapitulates RESTV infection as it is observed in cynomolgus macaques, although it exhibits more clinical hallmarks associated with the disease than the mouse model, suggesting that the ferret model may be a more appropriate model system for countermeasure evaluation and characterization of pathogenicity.

The humanized mouse model (hu-NSG-SGM3) is another rodent model used for studying filovirus infections. A recent study comparing RESTV and EBOV infection in humanized mice, showed dissemination of RESTV in the liver and spleen but with limited viral replication and normal serum biochemistry, suggesting an absence of organ damage (Spengler et al., 2017). The authors suggested that suppression of RESTV replication in the liver and eventual clearance of the virus may have prevented the development of severe clinical disease in this model, and better reflected what may occur in RESTV-infected humans. This model stands in contrast to our ferret model, as well as the STAT1$^{-/-}$ mouse model and the NHP model, in which severe disease is observed.

The fact that RESTV causes severe disease in some animal models but not others, raises the question as to what constitutes an appropriate RESTV animal model in the first place. Should we focus on animal models that do not develop disease following RESTV infection (such as humanized mice and some other rodents), or should we focus on those that do (such as ferrets and NHPs)? The answer to this question is likely a matter of perspective. Model systems in which RESTV causes severe disease may be important for understanding general aspects of filovirus pathogenesis, as well as for testing pan-filovirus vaccines or therapeutics. Conversely, models that do not develop disease may not only be useful for understanding why the virus is apathogenic in humans, but they may also be useful for understanding what makes a filovirus pathogenic in the first place. Indeed, it will be interesting to see whether future work can leverage both the “apathogenic” models, such as humanized mice, as well as the ferret model to identify the viral or host factors that contribute to RESTV disease in nonhuman primates but not humans.

One key advantage of the ferret models of ebolavirus infection, including the RESTV model, is that wildtype viruses, as opposed to host-adapted viruses, can be used. All immunocompetent rodent models rely on rodent-adapted virus variants possessing several genomic mutations (Banadyga et al., 2016). The impact of the differences between host-adapted viruses and wild type virus with respect to the pathogenesis, transmission and treatment strategy of a virus remains understudied. It is worth noting, however, that deep sequencing of the RESTV genome revealed no mutations in virus isolated from a terminal (10 dpi) blood sample from ferret #1059 compared to the challenge virus stock (data not shown), indicating that the disease reported here was likely not caused by virus mutation or adaptation.

The 100% lethality, dissemination of virus into the vital organs, liver damage and shedding of high amounts of virus makes the ferret model the most suitable small animal for studying RESTV pathogenesis and antiviral therapeutics, although the STAT1$^{-/-}$ and humanized mouse models may prove valuable for studying certain aspects of disease. Despite the fact that RESTV infection is not lethal to humans (Miranda and Miranda, 2011), isolation of RESTV in pigs co-infected with PRRSV raises the possibility that a novel and potentially human-pathogenic variant may emerge from these common agricultural animals (Cantoni et al., 2016; Marsh et al., 2011; Miranda and Miranda, 2011; Pan et al., 2014). The factors that contribute to the low pathogenicity of RESTV in humans and the possibilities of the emergence of a human-pathogenic RESTV variant through adaptation in humans need to be investigated. Additionally, thanks to its uniform lethality, the RESTV ferret model will likely prove useful for evaluating pan-ebolavirus therapies *in vivo*.

## Author contributions

XQ conceived the study and designed experiments. SH, LB and XQ performed the animal experiments. FY, WZ, MNR performed in vitro experiments and analyzed data. BC and CEH performed the immunohistopathology experiment and analyzed the data. FY, SH, LB, CEH and XQ interpreted the data. FY, LB, CS, CEH and XQ wrote the manuscript. All authors declare no conflict of interest.

## Acknowledgements

This work was supported by Public Health Agency of Canada, and partially supported by grants from the National Institutes of Health (U19AI109762-1). Authors would like to thank Mr. Kevin Tierney for assistance with animal experiments.

## Appendix A. Supplementary data

Supplementary data to this article can be found online at https://doi.org/10.1016/j.antiviral.2019.03.001.

## References


Albarino, C.G., Wiggleton Guerrero, L., Jenks, H.M., Chakrabarti, A.K., Ksiazek, T.G., Rollin, P.E., Nichol, S.T., 2017. Insights into Reston virus spillovers and adaption from virus whole genome sequences. PLoS One 12, e0178224.

Banadyga, L., Dolan, M.A., Ebihara, H., 2016. Rodent-adapted filoviruses and the molecular basis of pathogenesis. J. Mol. Biol. 428, 3449–3466.

Banadyga, L., Wong, G., Qiu, X., 2018. Small animal models for evaluating filovirus countermeasures. ACS Infect. Dis. 4, 673–685.

Barrette, R.W., Metwally, S.A., Rowland, J.M., Xu, L., Zaki, S.R., Nichol, S.T., Rollin, P.E., Towner, J.S., Shieh, W.J., Batten, B., Sealy, T.K., Carrillo, C., Moran, K.E., Bracht, A.J., Mayr, G.A., Sirios-Cruz, M., Catbagan, D.P., Lautner, E.A., Ksiazek, T.G., White, W.R., McIntosh, M.T., 2009. Discovery of swine as a host for the Reston ebolavirus. Science 325, 204–206.

Burk, R., Bollinger, L., Johnson, J.C., Wada, J., Radoshitzky, S.R., Palacios, G., Bavari, S., Jahrling, P.B., Kuhn, J.H., 2016. Neglected filoviruses. FEMS Microbiol. Rev. 40, 494–519.

Cantoni, D., Hamlet, A., Michaelis, M., Wass, M.N., Rossman, J.S., 2016. Risks posed by Reston, the forgotten ebolavirus. mSphere 1.

Centers for Disease Control, 1990. MMWR. Morbidity and mortality weekly report. Update: Filovirus Infection in Animal Handlers, vol. 39. pp. 221.

Cross, R.W., Mire, C.E., Borisevich, V., Geisbert, J.B., Fenton, K.A., Geisbert, T.W., 2016. The domestic ferret (Mustela putorius furo) as a lethal infection model for 3 species of ebolavirus. J. Infect. Dis. 214, 565–569.

de Wit, E., Munster, V.J., Metwally, S.A., Feldmann, H., 2011. Assessment of rodents as animal models for Reston ebolavirus. J. Infect. Dis. 204 (Suppl. 3), S968–S972.

Enkirch, T., von Messling, V., 2015. Ferret models of viral pathogenesis. Virology 479–480, 259–270.

Geisbert, T.W., Jahrling, P.B., 1990. Use of immunoelectron microscopy to show Ebola virus during the 1989 United States epizootic. J. Clin. Pathol. 43, 813–816.

Hayes, C.G., Burans, J.P., Ksiazek, T.G., Del Rosario, R.A., Miranda, M.E., Manaloto, C.R., Barrientos, A.B., Robles, C.G., Dayrit, M.M., Peters, C.J., 1992. Outbreak of fatal illness among captive macaques in the Philippines caused by an Ebola-related filovirus. Am. J. Trop. Med. Hyg. 46, 664–671.

Jahrling, P.B., Geisbert, T.W., Dalgard, D.W., Johnson, E.D., Ksiazek, T.G., Hall, W.C., Peters, C.J., 1990. Preliminary report: isolation of Ebola virus from monkeys imported to USA. Lancet 335, 502–505.

Jahrling, P.B., Geisbert, T.W., Jaax, N.K., Hanes, M.A., Ksiazek, T.G., Peters, C.J., 1996. Supplementum In: Experimental Infection of Cynomolgus Macaques with Ebola-Reston Filoviruses from the 1989-1990 U.S. Epizootic. Archives of Virology, vol. 11. pp. 115–134.

Jayme, S.I., Field, H.E., de Jong, C., Olival, K.J., Marsh, G., Tagtag, A.M., Hughes, T., Bucad, A.C., Barr, J., Azul, R.R., Retes, L.M., Foord, A., Yu, M., Cruz, M.S., Santos, I.J., Lim, T.M., Benigno, C.C., Epstein, J.H., Wang, L.F., Daszak, P., Newman, S.H., 2015. Molecular evidence of Ebola Reston virus infection in Philippine bats. Virol. J. 12, 107.

Kozak, R., He, S., Kroeker, A., de La Vega, M.A., Audet, J., Wong, G., Urfano, C., Antonation, K., Embury-Hyatt, C., Kobinger, G.P., Qiu, X., 2016. Ferrets infected with Bundibugyo virus or Ebola virus recapitulate important aspects of human filovirus disease. J. Virol. 90, 9209–9223.

Kroeker, A., He, S., de La Vega, M.A., Wong, G., Embury-Hyatt, C., Qiu, X., 2017. Characterization of Sudan Ebolavirus infection in ferrets. Oncotarget 8, 46262–46272.

Kuhn, J.H., Becker, S., Ebihara, H., Geisbert, T.W., Johnson, K.M., Kawaoka, Y., Lipkin, W.I., Negredo, A.I., Netesov, S.V., Nichol, S.T., Palacios, G., Peters, C.J., Tenorio, A., Volchkov, V.E., Jahrling, P.B., 2010. Proposal for a revised taxonomy of the family Filoviridae: classification, names of taxa and viruses, and virus abbreviations. Arch. Virol. 155, 2083–2103.

Marsh, G.A., Haining, J., Robinson, R., Foord, A., Yamada, M., Barr, J.A., Payne, J., White, J., Yu, M., Bingham, J., Rollin, P.E., Nichol, S.T., Wang, L.F., Middleton, D., 2011. Ebola Reston virus infection of pigs: clinical significance and transmission potential. J. Infect. Dis. 204 (Suppl. 3), S804–S809.

Miranda, M.E., Miranda, N.L., 2011. Reston ebolavirus in humans and animals in the Philippines: a review. J. Infect. Dis. 204 (Suppl. 3), S757–S760.

Miranda, M.E., White, M.E., Dayrit, M.M., Hayes, C.G., Ksiazek, T.G., Burans, J.P., 1991. Seroepidemiological study of filovirus related to Ebola in the Philippines. Lancet 337, 425–426.

Pan, Y., Zhang, W., Cui, L., Hua, X., Wang, M., Zeng, Q., 2014. Reston virus in domestic pigs in China. Arch. Virol. 159, 1129–1132.

Rollin, P.E., Williams, R.J., Bressler, D.S., Pearson, S., Cottingham, M., Pucak, G., Sanchez, A., Trappier, S.G., Peters, R.L., Greer, P.W., Zaki, S., Demarcus, T., Hendricks, K., Kelley, M., Simpson, D., Geisbert, T.W., Jahrling, P.B., Peters, C.J., Ksiazek, T.G., 1999. Ebola (subtype Reston) virus among quarantined nonhuman primates recently imported from the Philippines to the United States. J. Infect. Dis. 179 (Suppl. 1), S108–S114.

Siragam, V., Wong, G., Qiu, X.G., 2018. Animal models for filovirus infections. Zool. Res. 39, 15–24.

Spengler, J.R., Saturday, G., Lavender, K.J., Martellaro, C., Keck, J.G., Nichol, S.T., Spiropoulou, C.F., Feldmann, H., Prescott, J., 2017. Severity of disease in humanized mice infected with Ebola virus or Reston virus is associated with magnitude of early viral replication in liver. J. Infect. Dis. 217, 58–63.

World Health Organization, 1992. Viral haemorrhagic fever in imported monkeys. Wkly. Epidemiol. Rec. 67, 142–143.

Yuan, J., Zhang, Y., Li, J., Zhang, Y., Wang, L.F., Shi, Z., 2012. Serological evidence of ebolavirus infection in bats, China. Virol. J. 9, 236.